PROCEEDINGS, 48th Workshop on Geothermal Reservoir Engineering
Stanford University, Stanford, California, February 6-8, 2023
SGP-TR-224

Applications of Radial Jet Drilling Techniques in Geothermal Wells

Ramadan M. Ahmed and Catalin Teodoriu

100 E. Boyd Street, SEC 1210, Norman, OK 73019, USA

r.ahmed@ou.edu

Keywords: Radial Drilling, Stimulation, Magmatic Formation, Lateral Holes, Jetting

ABSTRACT

Developing geothermal reservoirs as enhanced geothermal systems (EGS) is becoming increasingly popular as a renewable energy resource. Hydraulic fracturing improves the permeability of these resources by stimulating their reservoirs. Nevertheless, creating controllable fractures in deep geothermal wells can be challenging because the rocks are strong and their crystal structure is intact. Radial Jet Drilling (RJD), which creates microholes through the rock, could effectively stimulate geothermal reservoirs. RJD is an emerging technology that utilizes high-pressure water to drill several radial holes from an existing vertical well. The technique has been developed for stimulating oil and gas wells. It provides unique features required for effective reservoir stimulation.

There is evidence that RJD could increase oil and gas production by more than fivefold. However, in geothermal wells, its applications are limited due to the challenge of jetting hard magmatic formations. Even though successful jetting of hard rocks was performed under atmospheric conditions, field tests demonstrated the challenge of drilling laterals in geothermal wells. Thus, further research is needed to advance RJD for use in geothermal wells with hard rock formations.

The purpose of this article is to review recent RJD studies conducted to stimulate geothermal wells. Globally, various efforts have been made to adapt RJD to exploit geothermal resources in recent years. Several factors affect RJD technology's effectiveness, including jetting bit design, fluid composition and properties, circulation rate, injection pressure, stress state in the formation, borehole pressure, and temperature. These factors determine performance parameters such as penetration rate and propulsion force. The RJD operation requires a high rate of penetration (ROP) to drill at an economical rate, while propulsion force is needed to propel the bit at the achieved ROP.

1. INTRODUCTION

Currently, doublet systems are created by drilling injection and production wells to extract geothermal energy. The system produces hot water or steam from the production well by injecting water into the injection well. Hence, the system requires an effective connectivity between the two wells. To efficiently harvest the geothermal heat, the injected fluid must flow from the injection well to the production well through the reservoir in a controlled manner, either through the original permeability of the formation or through fractures. The formations of deep geothermal reservoirs often have low permeability; therefore, fractures, either natural or man-made, are necessary to enhance fluid flow and heat extraction. By creating high permeability fractures (flow paths), enhanced geothermal systems (EGS) improve the reservoir's natural permeability. Hydraulic fracturing is the traditional method of creating fractures. Nonetheless, fracturing operations have been limited by the challenges of creating controllable fractures (in particularly controlling their direction) and associated seismic activities. Therefore, RJD can be used to stimulate geothermal wells if its technical limitations are overcome. Compared to conventional hydraulic fracturing, RJD provides several advantages, such as minimal induced seismicity, reduced water requirements, better control over the direction and length of the created flow path, and reduced cost (Salimzadeh et al. 2019). As a result, RJD has the potential to become an alternative to hydraulic fracturing for EGS.

According to Goryschny et al. (2015), fishbone drilling (a version of RJD that implies a multitude of microholes) can mitigate the need for hydraulic fracturing in tight gas reservoirs where hydraulic fracturing can cause seismic activity. The primary goal was to ensure the calculated (pseudo-steady state) production rate remained constant for the first year. Favorable economic results obtained from the study demonstrated fishbone drilling is an attractive alternative to hydraulic fracturing.

The RJD technology has been developed in the oil and gas industry to mitigate near-wellbore formation damage. The technique involves typically two steps: milling a window and drilling a lateral hole. In the first step, a diverter is run into the hole and positioned at the desired depth. A tool is then run in a hole to mill a window through the casing. In the second step, a jetting assembly (jetting bit and flexible tube) is lowered into the well and oriented to the milled window. The water pressure is then increased to circulate fluid through the bit and create a strong jet that can drill a lateral hole through the rock. Without a rigid drill string, the axial force cannot be transferred to the bit as it penetrates the formation. Hence, the bit is driven by hydraulic means. Therefore, strong back-jetting is required to offset the recoil force created by the front jetting and advance the bit forward against other resistive forces, such as mechanical friction and hydrodynamic forces developed due to the flow around the flexible tube (Wiechman and Ahmed 2018; 2022).

The lateral hole drilling using RJD, which has directional control, is expected to effectively stimulate EGS by connecting the wells to the natural fractures of the reservoir. A recent finite element-based simulation study (Salimzadeh et al. 2019) predicted the expected improvement in heat production due to RJD laterals in high-fracture-density geothermal reservoirs, even though no significant effect on the injectivity or productivity is anticipated. In reservoirs with low matrix permeability, the RJD laterals are expected to connect the wells

to the fracture network and improve the well performance and compensate for the lack of directional control of hydraulic fracturing, especially due to stress shadowing. Also, in situations where the wells are not connected directly to the fractures, the length of RJD laterals is anticipated to play a vital role in enhancing the energy production rate. These simulation results are consistent with an RJD study (Nair et al. 2017) conducted on geothermal wells. Despite RJD's numerous advantages, it also has several limitations and challenges compared to conventional hydraulic fracturing. In addition, geothermal resources may present more severe challenges. The typical limitations and challenges of RJD include the following:

- It requires high-performance equipment, such as pressure intensifiers, to reach high jet speeds and hydraulic power.
- Flexible tubing with high-pressure ratings is essential.
- Various factors influence lateral length, including bit design, rock properties, and operating parameters.
- Directional control and surveillance operations are challenging.
- The challenge of optimizing rock-breaking efficiency, lateral length, and bit hydraulics.

2. RECENT ADVANCES

2.1 Rock Hardness and Jetting Requirement

According to some studies, RJD could improve oil and gas production fivefold from existing wells. Also, some RJD operations have successfully drilled geothermal wells in sedimentary basins. Nonetheless, high-pressure jetting at high flow rates is required to jet hard rocks, which limits the application of RJD in hard magmatic formations. Despite the effective jetting of hard rocks in the open air (atmospheric conditions), drilling laterals in hard formations proved challenging under confined pressure. In addition to the jetting bit's design and operating conditions, the characteristics of the rock and stress conditions in the formation also affect the success of the jetting operation (Stoxreiter et al. 2018). In general, it seems easier to jet in the direction of the minimum principal stress than in the direction of the maximum principal stress. The work of Stoxreiter et al. (2018) conducted on jet-assisted rotary drilling presented a very important piece of information that can be used in overcoming the limitation of RJD. The study examined the jetting requirement for different rocks under various operating conditions. Experiments under different ambient conditions were carried out to study the cutting actions of fluid jets in hard rock formations. A variety of core samples were tested under atmospheric conditions to determine the jettability of various hard rock formations. For a realistic simulation of deep downhole conditions, a pressure vessel capable of 450 bar of internal pressure was built. Experimental results show that cutting performance under different ambient pressure conditions is entirely different from that under atmospheric conditions (**Fig. 1a**). Several factors influencing performance were identified and adapted to ensure good performance in all experimented scenarios. The use of drilling fluids instead of water was also investigated. According to the investigation, high-pressure jetting is achievable under simulated downhole conditions. The conditions include high ambient pressures, jets of varying pressures acting concurrently, drilling fluid as a surrounding medium, and high jet velocity.

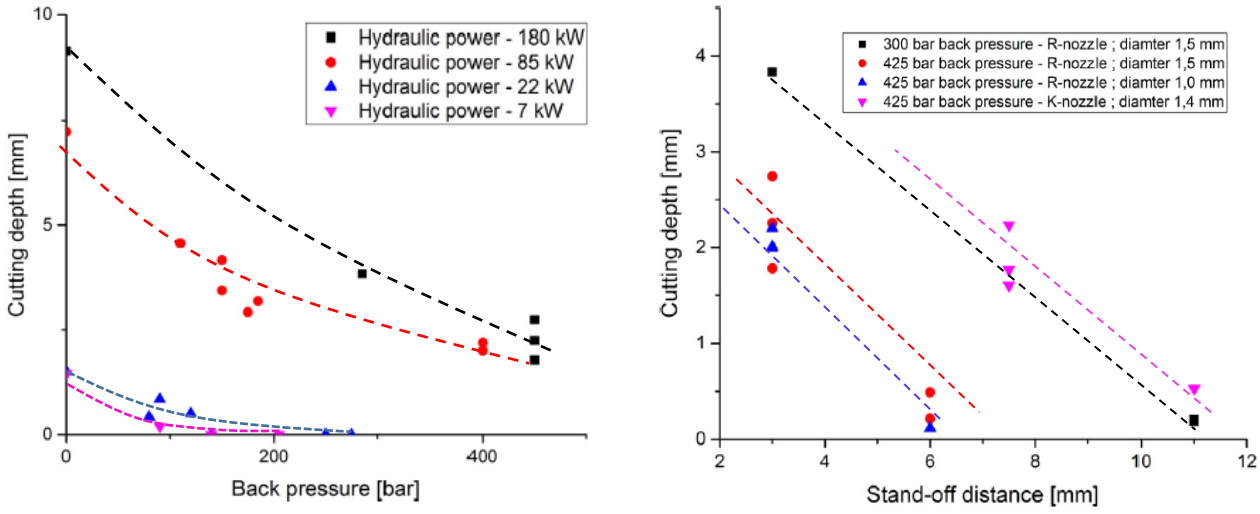

Fig 1: Drilled depth as a function of: a) confining pressures; and b) stand-off distance (Stoxreiter et al. 2018)

RJD operations require identifying the jetting parameters that yield good cutting performance under high confining pressures. Previous studies (Cheung and Hurlburt 1979 and Kolle 1987) have shown that the standoff distance (distance between the rock surface and the nozzle's tip) determines the nozzle's performance. It is possible to have a high standoff under atmospheric conditions as the hydrodynamic drag generated by the surrounding fluid can be smaller than the one developed by viscous fluids like water. Furthermore, the diversion (spreading) of the jet also reduces its effectiveness, besides the drag effect. Under downhole conditions with pressurized water as the surrounding fluid, the confined compressive strength of the material increases, and the standoff distance becomes a limiting factor if the jetting bit is not properly propelled. According to earlier studies (Kolle 1987 and Schlichting and Gersten 1997), the jet drilling action ceases at a distance of 6.57 times the nozzle diameter. Therefore, for successful implementation of RJD in hard geothermal formations, the jetting nozzle must rapidly advance while drilling the hole to reduce the standoff distance between its tip and the rock surface. Figure 1b shows the maximum depth of holes drilled at different standoff distances and confining pressures (back pressures). These measurements were obtained by jetting granite rocks with water at 2500 bar jet pressure. The results reasonably agree with the proposed maximum standoff distance. In the case of a 1.4 mm nozzle, the maximum gap between the nozzle outlet and the rock surface was 11 mm, and the

predicted distance was 9.2 mm. As shown in Fig. 1a, confining pressure affects drilling depth at varying levels of bit hydraulic power. The results showed that confining pressure significantly reduced jet performance. Furthermore, the drilled depth varied with the type of nozzle as well as the hydraulic power provided to the bit (Stoxreiter et al. 2018)

2.2. Jetting Performance

In the RJD technique, there is a strong correlation between equipment capabilities (maximum flow rate and pressure), jetting bit design The RJD technique strongly correlates equipment capabilities (flow rate, pressure, and fluid type), jetting bit design (nozzle size, geometry, and configuration), lateral length, and rock-breaking efficiency that could directly affect the drilling performance. Flow rate and pressurization capabilities of the RJD system directly affect hydraulic power generated at the bit. Hard rocks require high injection pressure, flow rate, and hydraulic power. Using a high-pressure water jet to drill rock is much more complex than a conventional rotary drill (Huang and Huang 2019).

Studies have shown that deep geothermal wells often contain hard rocks that require high-pressure jetting (more than 100 MPa). The hydraulic power provided by the pump is the energy source for the RJD system to drill the rock, propel the bit, and circulate the fluid in the system. The circulating pressure drop of an RJD system consists of five components: the pressure drop across the coiled tubing (CT), high-pressure flexible tube, jetting bit, lateral hole annulus, and primary wellbore annulus. The pressure drop across the jetting bit determines the hydraulic power and efficiency of the bit. Other components are parasite pressure losses, which must be minimized to optimize the process.

The RJD system also relies heavily on bit design. Therefore, improving the bit design is an excellent way to enhance rock-cutting efficiency. For instance, swirling multi-nozzle bits offer the best efficiency with the lowest specific energy (Li et al. 2017). Furthermore, they create more even and round lateral holes that have better hole stability than the ones drilled by non-rotating bits. However, their surface contact area is slightly lower due to their roundness. Furthermore, bit design parameters, including nozzle configuration, geometry, and size, are central in determining RJD performance. This is because these parameters directly control the bit impact and propulsion forces needed for drilling the rock and propelling the bit. Along with flow rate and injection pressure, these parameters also determine the penetration rate and maximum hole length achieved by RJD.

The type of jetting medium is another method to enhance drilling efficiency. Pulsed jets and abrasive jets effectively reduce the rock-cutting threshold pressure of the jet, which is required to drill hard rocks such as granite. Gasified jets are also a new rock-breaking approach, especially for hot-dry rocks (Zhang et al. 2018)

2.3. Trajectory Measurement and Control

Traditional surveying tools cannot be utilized in the RJD technique due to the short radius turning of the flexible tubing in the diverter and the small diameter of the laterals. Consequently, it remains impossible to determine and control the trajectory of lateral holes. As a result of the uncertainty in the trajectory, it is difficult to evaluate the performance of the jetting operations and predict production from them (Huang and Huang 2019). The diverter controls the hole's position, inclination, and azimuthal angle only at the entry point. After the entry point, the bit is assumed to advance straight forward. The trajectory, however, may differ from the straight line due to imbalances in forces and angular momentums due to the jetting process. In general, it limits the advancement of RJD technology and its application in the field. This issue has been the subject of few studies to date. Early tools (Balch et al. 2016; Dickinson et al. 1989) for obtaining well trajectory data still have some limitations such high hydraulic friction and errors in measuring hole length. Microchip technology can, however, improve RJD's well-path measuring method. As a result, the size of the tool is the primary limiting factor. Tool size must be small enough to pass through the diverter and narrow lateral holes. In addition to its measuring components, it requires a power unit and memory module that need additional space. Moreover, the tool's protective cover must be made of materials that are high-strength and non-magnetic. With microchip technology, a measuring tool with sensors, a power unit, and a memory module can be developed in a compact size.

A recent study (Reinsch et al. 2018) showed that acoustic monitoring could be used to estimate the location of nozzles. A three-component accelerometer and unidirectional piezo elements were used as monitoring instruments. The sensors were spaced 2 m apart along two lines that were roughly parallel to ground level. The piezo-elements and accelerometers were used to record the acoustic signal resulting from jetting action. Based on acoustic data, the bit position is calculated as a function of measured depth. Furthermore, three-dimensional (3D) accelerometers combined with 3D magnetic field sensors (magnetometers) were used to measure the trajectories of the holes in order to evaluate the accuracy of the acoustic method. A fiberglass rod was inserted into the hole with the sensors mounted on it. Azimuth and inclination measurements were taken every 25 cm while pulling out of the hole. Acoustic measurements were compared with accelerometer and magnetometer trajectory data. During the experiment, a flexible hose and various types of jetting bits were used to drill five lateral holes into a quarry wall (**Fig. 2**). The jetting was performed using a high-pressure pump with a capacity of 30 L/min at 1,000 bar. The study pointed out the following key findings:

- In terms of estimating the nozzle location, the acoustic monitoring approach was partially successful.
- The jetted holes don't follow a straight line.
- Rotating bits displayed the highest ROP values.
- The bit should be stabilized while jetting to minimize the curvature of the jetted hole.

There are no entirely straight trajectories among those measured. Each trajectory had a different curvature; some changed gradually, while others varied moderately. However, none of them showed a sharp turn. In **Figure 3**, all the trajectory projections are shown in two dimensions (2D). A magnetized metal pipe influenced the trajectory measurements of holes 1-3. Each hole's trajectory appeared to diverge

upward over its length. Eventually, even the one originally pointing downward (hole 6) changed direction. Similarly, all hole trajectories diverted to the west side in the east-west direction. Hole 6 was drilled using a rotating bit. Therefore, bit asymmetric design effects are expected to be minimal. The most likely explanation for this observation is that the formation properties change in the upper section. The jet was drilling faster in the soft side of the rock. Due to the flexibility of the hose and bit propulsion behavior, the bit follows the trajectory of the hole.

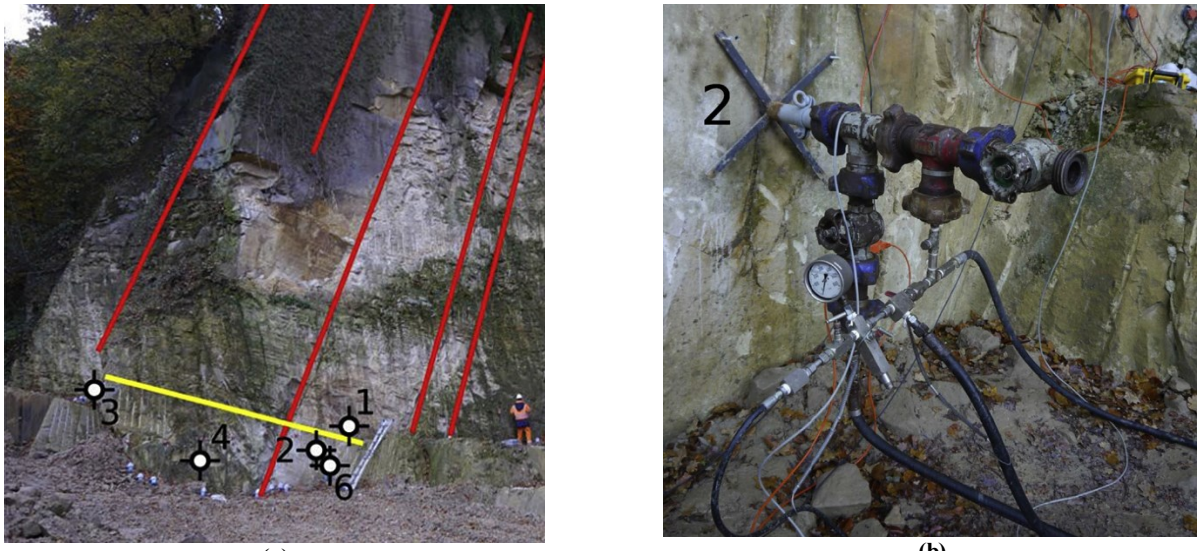

(a) **(b)**

Fig 2: Quarry wall (a); and wellhead (b) (Reinsch et al. 2018)

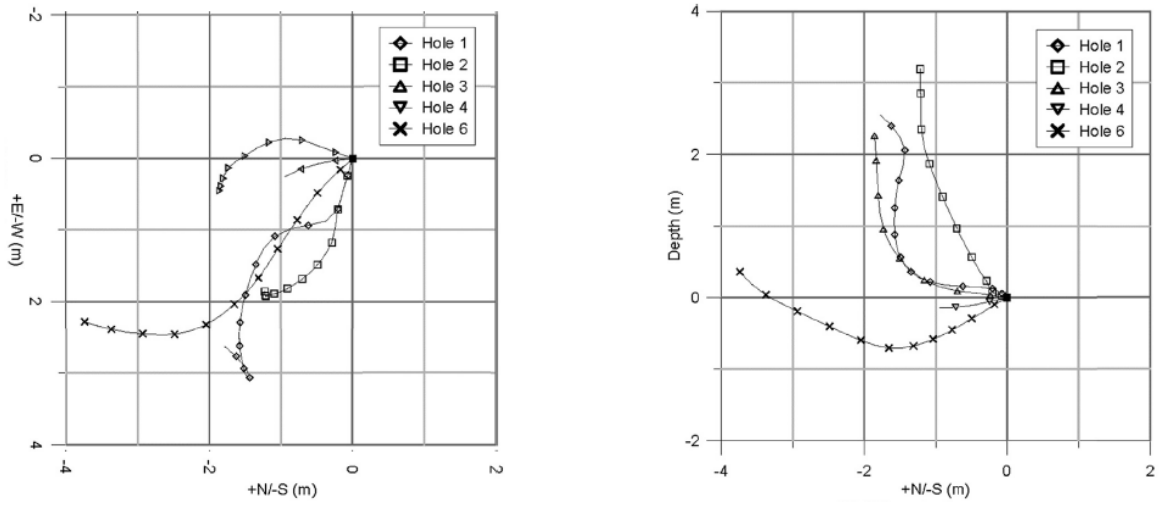

(a) **(b)**

Fig 3: Trajectories of lateral holes: a) plane view; and b) side view (Reinsch et al. 2018)

A digital camera mounted on a fiberglass rod was used to inspect each hole (Reinsch et al. 2018). Every hole was photographed until the camera could not advance deeper into the hole or a narrow spot prevented it from doing so. Over a significant interval, each hole's diameter exceeded 20 mm. In addition, some hole intervals showed star-shaped profiles caused by the backward-jetting nozzles. Three fractures were intersected during jetting. The angles at which fractures were intersected varied from approximately 25 to almost 90 degrees (**Fig. 4**). Observations of iron-manganese minerals were made on fracture faces (Fig. 4b). A larger excavated volume was observed before the 90 fracture, indicating a harder fracture face. The weaker sandstone side was eroded without penetrating the fracture face. This observation supports the previous explanation of jetting direction change caused by altered formation properties. The jets drilled faster through the softer side of the formation, causing a consistent upward change in direction.

(a) (b) (c)

Fig 4: Photographs of holes with fracture with different intersection angles: a) 45°, b) 90°, and c) 25° (Reinsch et al. 2018)

3. HYDRAULIC MODELING

A variety of factors affect the performance of an RJD bit, including formation characteristics, jetting fluid properties, and cutting and propulsion forces. Jetting bits with forward nozzles generate cutting forces using fluid discharged at high velocity (Dickinson and Dickinson 1985). The nozzles (**Fig. 5**) are often treated as small-diameter thick orifices for mathematical analysis. Discharge coefficients, which account for abrupt flow geometry changes in the bit, are thus a performance-limiting parameter in designing the jetting bits. There are many factors to consider when optimizing cutting force, including the number of nozzles, nozzle diameter, deviation angles, jet velocity, and pressure differential. Many of these factors also affect the propulsion force. Also, the thrust force generated by back-jetting nozzles must overcome the recoil force generated by the front-jetting nozzles to penetrate the rock formation. The bit cannot advance otherwise. The back-jetting advances the bit and increases hole size while simultaneously removing cuttings.

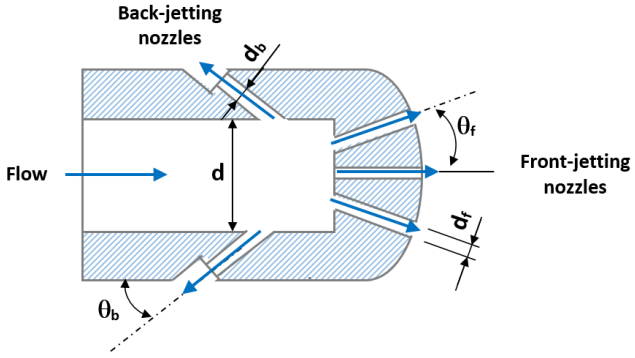

Fig. 5: Multi-nozzle jetting bit design (redrawn from Chi et al. 2016)

3.1. Model Assumptions and Formulations

The discharge coefficient correlations have recently been incorporated in modeling the RJD hydraulics (Wiechman and Ahmed 2018; 2022). The model considers various simplifying assumptions, including steady-state and isothermal flow conditions, incompressible fluid, cleaned lateral hole without cutting accumulation, flexible tubing, jetting bits with symmetric design, and smooth, straight, and defectless nozzles. Furthermore, the model uses an empirical discharge coefficient correlation to determine the jet velocity (V_n) accurately. Thus, the jet velocity achieved in front-jetting nozzles is computed as follows:

$$V_{n,i} = C_{df,i}\sqrt{2\Delta P_b/\rho} \tag{1a}$$

where ΔP_b is the bit pressure drop, and ρ is the fluid density. $V_{n,i}$ and $C_{df,i}$ are the jet velocity and discharge coefficient of the front-jetting nozzle i. For back-jetting nozzle k, a similar equation can be written as follows:

$$V_{n,k} = C_{db,k}\sqrt{2\Delta P_b/\rho} \tag{1b}$$

The discharge coefficient of front-jetting nozzles with aspect ratios ($a_i = L_i/d_{n,i}$) ranging from 0.to 2.5 is determined using the following equation, where $d_{n,i}$ and L_i depict the diameter and length of the nozzles.

$$C_{df,i} = -0.0573a_i^2 + 0.2338a_i + 0.575 \tag{2a}$$

For large aspect ratios ($2.5 < a_i \leq 9.0$), the discharge coefficient is determined as:

$$C_{df,i} = 0.292[1 + a_i^{-0.068}] + \frac{0.292}{(1+a_i)^{0.150}} \quad (2b)$$

Discharge coefficient formulas displayed in Eqns. (2) are developed for front-jetting nozzles. Recent measurements, however, revealed that back-jetting nozzles have a discharge coefficient value that is 16% lower than front-jetting nozzles. Thus: $C_{db,i} = 0.84 C_{df,i}$.

Applying the conservation of mass and utilizing the jet velocity equations, the total flow rate (Q) can be related to the bit pressure drop as follows:

$$\Delta P_b = \frac{\rho Q^2}{2\left(\sum_{i=1}^{N} A_i\, C_{df,i} + \sum_{k=1}^{M} A_k\, C_{db,k}\right)^2} \quad (3)$$

where A_i and A_k are the cross-section areas of jetting nozzles i and k, respectively. Jetting of the lateral holes is successfully conducted when the jet strikes the end of the hole at a maximum velocity that creates strong impact force and high localized stress in the rock due to increased stagnation pressure. The total jet impact force (F_j) generated by the front nozzles can be calculated as:

$$F_j = \sum_{i=1}^{N} \rho V_{n,i}^2 A_i \quad (4)$$

where N is the total number of front nozzles on the jetting bit. Besides the impact force, the hydraulic power is vital parameter to optimize bit performance. The total hydraulic power of the bit (P_T) is calculated as:

$$P_T = Q * \Delta P_b \quad (5)$$

A reaction force is generated as high-speed jets exit the nozzles. Since the nozzles deviate, the reaction forces have both axial and lateral components. The axial component of these forces tends to recoil the bit backward. Accordingly, the total recoil force acting on the bit due to i is:

$$F_R = \sum_{i=1}^{N} \rho V_{n,i}^2 A_i Cos(\theta_{f,i}) \quad (6)$$

where A_i and $\theta_{f,i}$ are the cross-section area and deviation angle of front nozzle i. An opposite and higher thrust is required to propel the bit into the drilled hole. The back-jetting nozzles create the thrust necessary to advance the bit forward. The total thrust force (F_T) advancing the bit forward is computed as:

$$F_T = \sum_{k=1}^{M} \rho V_{n,k}^2 A_k Cos(\theta_{b,k}) \quad (7)$$

where M is the number of back-jetting nozzles existing on the bit. The propulsion force is the resultant of these two forces. Therefore, it is computed as:

$$F_P = \sum_{k=1}^{M} \rho V_{n,k}^2 A_k Cos(\theta_{b,k}) - \sum_{i=1}^{N} \rho V_{n,i}^2 A_i Cos(\theta_{f,i}) \quad (8)$$

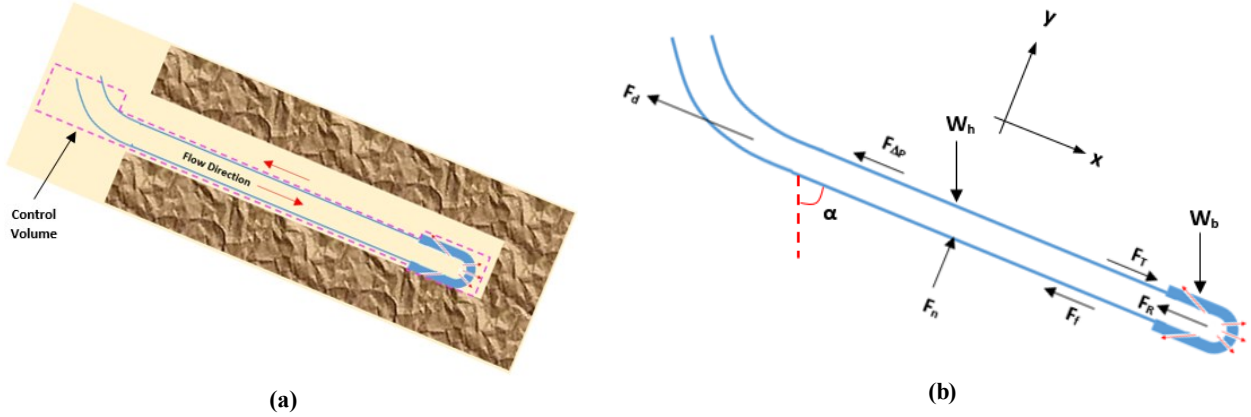

(a) (b)

Fig. 6: Radial drilling string in an inclined lateral hole (a); and it free-body diagram (b)

Since a flexible tube is used as a drill string, the axial force cannot be transferred. According to the control volume in the free body diagram presented in **Fig. 6**, the momentum balance of the drill string in the axial direction (x-axis) is given by:

$$\sum F_x = \left(\sum_{k=1}^{M} \dot{m}_k V_{x,k} + \sum_{i=1}^{N} \dot{m}_i V_{x,i}\right)_{out} - \left(\sum_{k=1}^{M} \dot{m}_k V_{x,k} + \sum_{i=1}^{N} \dot{m}_i V_{x,i}\right)_{in} \quad (9)$$

where $\dot{m}_i$ is the mass flow rate and $V_{x,i}$ and $V_{x,k}$ the axial component of the velocity of the fluid entering or exiting the control volume at the inlets and outlets. High-pressure jetting is needed for magmatic formations present in geothermal reservoirs. However, high pressure requires tubes with a thicker wall or made of a stronger material, which increases diverter friction. Due to the burden tube effect, high pressure also increases friction force. For geothermal applications with excessive jetting pressure, inclined laterals are more appropriate.

The momentum equation (Eq. 9) can be specifically written for the lateral drill string considering the axial component of the momentum flux of fluid entering the control volume, mechanical friction, the axial component of gravitational forces, and hydraulic force caused by the annular pressure gradient ($F_{\Delta P}$) acting on the drill string. Therefore:

$$-F_f - F_d - F_{\Delta P} + W_T \cos(\alpha) + W_b \cos(\alpha) = \sum_{i=1}^{N} \rho V_{n,i}^2 A_i Cos\left(\theta_{f,i}\right) - \sum_{k=1}^{M} \rho V_{n,k}^2 A_k Cos(\theta_{b,k}) \tag{10}$$

where F_f and F_d are the static friction force between the tube and hole and the friction force in the diverter, respectively; $F_{\Delta P}$ is pressure gradient force that oppose the advancement of the bit. W_T and W_b are the effective weight of the tubing and the jetting bit that are expressed as:

$$W_T = g\frac{\pi}{4}\left(D_o^2 - D_i^2\right)(\rho_T - \rho)L \tag{11}$$

$$W_b = m_b g\left(1 - \frac{\rho}{\rho_b}\right) \tag{12}$$

where D_o and D_i the outer and inner diameters of the tube. ρ_b and ρ_T are the densities of the bit and the tube. m_b is the mass of the bit in air. L is the length of the lateral. By representing momentum fluxes with equivalent recoil and trust forces, the following force balance equation can be formulated. A free-body diagram (Fig. 6b) of the radial drilling string shows where and how these forces are acting.

$$-F_f - F_d - F_{\Delta P} + W_T \cos(\alpha) + W_b \cos(\alpha) = F_R - F_T \tag{13}$$

Diverter friction is found by Bin et al. (2016) to be proportional to the difference between the internal and external pressures of the tube, according to experimental measurements. Therefore, an empirical model was developed to calculate the friction in diverters. However, the model's applicability is limited to the diverter design used in its development. The pressure gradient force is a function of the projection area of the bit (A_o), length of the lateral (L) and the annular pressure gradient $\left(\frac{dP}{dL}\right)$. Thus:

$$F_{\Delta P} = A_o\left(\frac{dP}{dL}\right)L \tag{14}$$

The annular friction pressure gradient can be determined using a hydraulic model presented by Wiechman and Ahmed (2022). Equation (13) can be more simplified applying the propulsion force and pressure gradient force expressions. Consequently:

$$F_f = F_P - F_d - A_o\left(\frac{dP}{dL}\right)L + W_T \cos(\alpha) + W_b \cos(\alpha) \tag{15}$$

As the flow rate increases, the propulsion force increases faster than the pressure gradient force, increasing the static friction. Upon reaching its maximum value, the friction force causes the string to advance. The maximum static friction ($F_{f.max}$) is calculated from the static friction coefficient (μ_{st}) and the normal force (F_n). Thus: $F_{f.max} = \mu_{st} F_n$. Considering the lateral forces shown in the free-body diagram (Fig. 6b), the normal force can be determined by applying momentum balance in the y-axis. Thus:

$$F_n = W_T \sin(\alpha) + W_b \sin(\alpha) \tag{16}$$

Equation (16) can be further simplified by applying the expressions of the effective weights of the tube and the bit presented in Eqs. (11) and (12). Thus:

$$F_n = \left[g\frac{\pi}{4}\left(D_o^2 - D_i^2\right)(\rho_h - \rho)L + m_b g\left(1 - \frac{\rho}{\rho_b}\right)\right]\sin(\alpha) \tag{17}$$

As the length of the tube increases, the normal force also grows linearly, making sliding difficult. As a result, the maximum drillable length is reached when $F_f = \mu_{st} F_n$. The maximum drillable lateral hole length can be obtained by combining Eqns. (11), (12), (15) and (17). Thus:

$$L_{max} = \left(\frac{F_P - F_d}{\mu_{st}} - B\emptyset\right) \Big/ \left(A\emptyset + \frac{A_o}{\mu_{st}}\left(\frac{dP}{dL}\right)\right) \tag{18}$$

where $\emptyset$ is a dimensionless parameter which is a function of friction coefficient and hole inclination angle measured from the vertical axis. The parameter mathematically expressed as:

$$\emptyset = \sin(\alpha) + \frac{\cos(\alpha)}{\mu_{st}} \tag{19}$$

3.2 Model Validation

Wiechman and Ahmed (2022) performed experiments with two jetting bits with one front and two back jetting nozzles to validate the new model. Also, experiments were conducted with jetting bits that didn't have back jetting nozzles (i.e., only single from the nozzle). Single-nozzle bits were re-machined to add back-jetting nozzles to perform multi-nozzle tests. The dimensions and geometric descriptions of the multi-nozzle bits are presented in **Table 1**. During the experiments, flow rates and propulsion forces were measured. **Figures 7** and **8** compare measurements and model predictions. Jet velocities were significantly lower than single nozzle bits due to the increased flow area. Stable flow rates were maintained throughout the experiment to establish steady-state flow conditions. A multi-nozzle bit's flow rate curve is similar to a single-nozzle bit's. The theoretical model predicts a linear increase in propulsion force with pressure drop. Measured trends confirm model predictions. The propulsion force and flow rate were predicted by the model reasonably well. The maximum discrepancy between model predictions and measured data is 33%.

Table 1: Descriptions of jetting bits (Wiechman and Ahmed 2022)

Bit #	Jetting Direction	Nozzle Diameter (mm)	Nozzle Length (mm)	Aspect ratio (-)	Deviation Angle
1	Front	0.893	2.30	2.58	0°
	Back	1.600	6.00	3.75	30°
2	Front	1.073	2.25	2.10	0°
	Back	1.600	6.00	3.75	30°

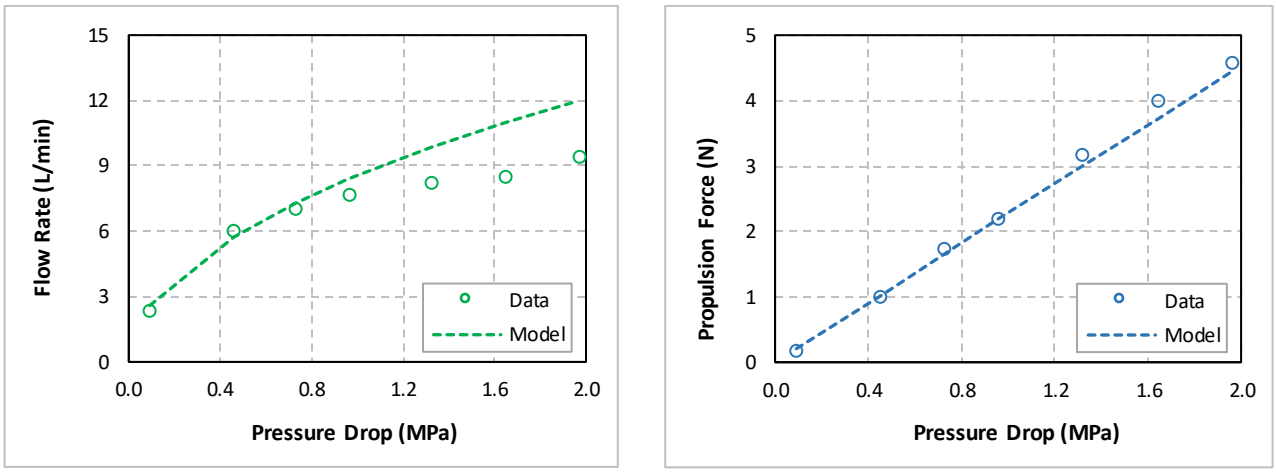

(a) (b)

Fig. 7: Results of Bit # 1: a) flow rate vs pressure drop; and b) propulsion force vs. pressure drop (Wiechman and Ahmed 2022)

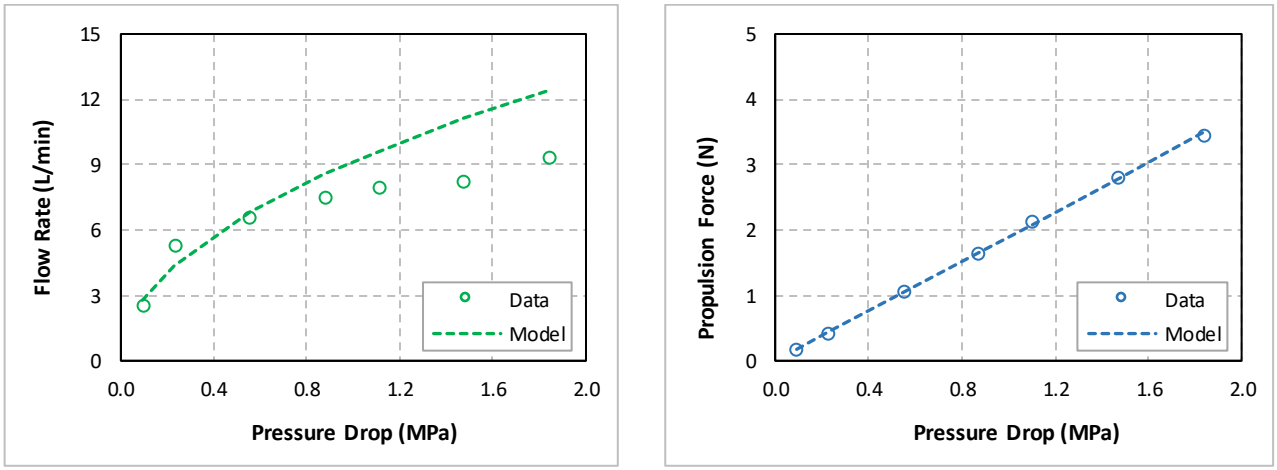

(a) (b)

Fig. 8: Results of Bit # 2: a) flow rate vs pressure drop; and b) propulsion force vs. pressure drop (Wiechman and Ahmed 2022)

As the pressure drop increases, model predictions deviate from the data. There is a tendency for discrepancies to occur when bits have small nozzles, as shown in Figs. 7 and 8. Manufacturing defects can lead to an increase in differences in this scenario since machining defects such as nozzle wall-roughness, deviation angle, and straightness were more pronounced with decreasing nozzle diameters. Due to the increase in pressure drop, these defects reduced the flow rate as the Reynolds number increased. This observation is analogous to turbulent flow in pipes, where pipe wall roughness significantly impacts small pipes' hydraulic resistance more than large pipes'. The model provides better propulsion force forecasts despite these noticeable discrepancies in flow rate, with a maximum discrepancy of 15%.

Additionally, the most remarkable difference between measurements and predictions was observed during experiments in which force measurements were within the instrument's accuracy range (Fig. 7b).

3.3 Sensitivity Analysis

This sensitivity analysis investigates how wellbore friction coefficients, hole diameters, hose density, and diameters of back-jetting nozzles influence the maximum hole length (MHL). The analysis is based on a field case study presented by Bin et al. (2016). They studied the effect of a 9+5+1 bit design, which contains nine back-jetting nozzles of 0.9 mm with a deviation angle of 30°, five front-jetting nozzles of 0.7 mm with a deviation angle of 12°, and one front-jetting nozzle without a deviation angle (center nozzle) of 0.7 mm. In addition to these parameters, **Table 2** shows other input parameters used in the baseline case.

Table 2: Baseline case input parameters for sensitivity analysis (Wiechman and Ahmed 2022)

Fluid density	1000 kg/m³		Friction factor/coefficient	0.35
Tube/Hose Density	1800 kg/m³		Friction in the diverter	0.0 N
Bit Density	7800 kg/m³		Aspect ratio of front nozzles	2.0
Tube/Hose outer diameter	14 mm		Aspect ratio of back nozzles	2.0
Tube/Hose inner diameter	9 mm		Hole diameter	40 mm
Mass of the bit	0.5 kg		Hole roughness	0.3 mm

Figure 9 illustrates how various factors influence the MHL, one of the performance parameters of the jetting bit. This wellbore length balances propulsion forces with resistance forces. Resistance forces considered in this analysis are mechanical friction and pressure gradient force. The sensitivity of MHL was evaluated by varying selected parameters with fixed increments from baseline values (±10%, ±15%, ±20%, and ±30%). The MHL increases when the friction coefficient is reduced, as expected (Fig. 9a). A decrease in MHL is also caused by an increase in friction coefficient. In spite of this, its impact is slightly less than its reduction. This particular case shows a moderate effect of friction coefficient. Wellbore quality (cleanliness, roughness, and straightness), the tube/hose material's physical properties, and fluid lubricity all influence the friction coefficient between the wellbore and the tube/hose. By selecting the right tube/hose material and drilling fluid and taking care of wellbore quality issues, friction can be minimized, and improvement in MHL can be achieved.

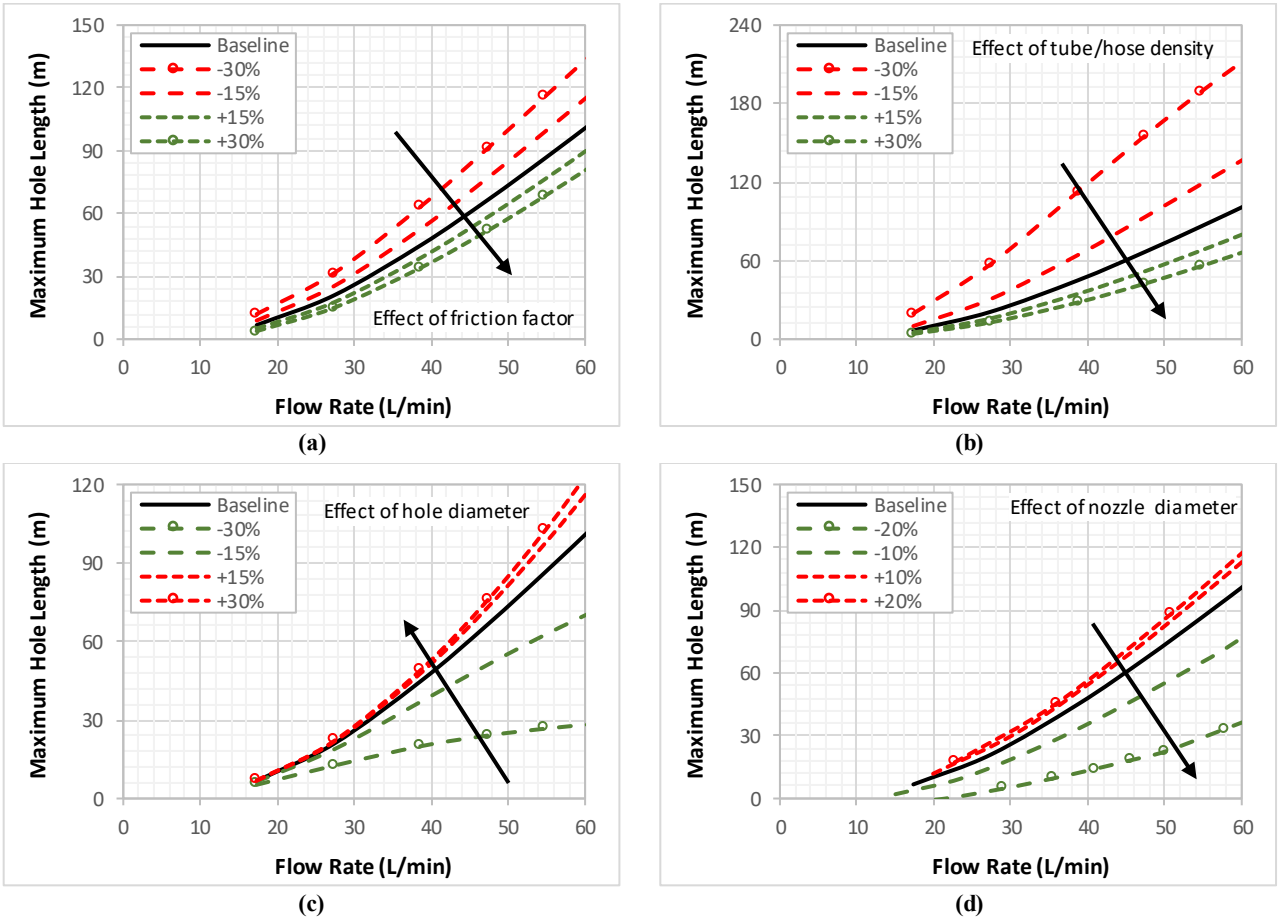

Fig. 9: Effects of changing nozzle diameter on various performance parameters: a) pressure drop, b) bit hydraulic power, c) propulsion force, and d) maximum hole length (Wiechman and Ahmed 2022)

Another important parameter affecting MHL is the tube/hose density. MHL is reduced significantly (Fig. 9b) by increasing the density of the tube, especially at low tube densities (less than 1800 kg/m3). In nonmetallic low-density hoses, tube density is more important. Aluminum and titanium-based alloys can be used to improve MHL in metallic tubes. Stainless steel, for example, requires significantly higher propulsion force than less dense metals. In this case, more flow will go to the back-jetting nozzles, limiting the jetting capability of the front nozzles and reducing penetration rates. Furthermore, a reduction in front jet velocity prevents the bit from drilling hard rocks.

Several factors determine the size of the hole, including the jetting bit size, the number of jetting nozzles, and the angle of deviation of the front and back-jetting nozzles. MHL is significantly affected by hole diameter (Fig. 9c). Maintaining high MHL can be achieved by selecting the appropriate number of nozzles, nozzle size, deviation angle, and fluid circulation rate, as well as the desired hole diameter. Maintaining a clean wellbore and drilling holes without irregularities will also reduce excess pressure losses and the associated resistance forces. To clean the lateral with a back-jetting nozzle, most field operators make frequent wiper trips while drilling. Since the jet velocity is normally high, the cleaning is more effective. Due to the ease of making quick trips, cleaning lateral holes is not a major problem, despite limited circulation. Additionally, MHL is more affected by hole diameter as the flow rate increases. This is because hole diameter influences annular fluid velocity, which in turn controls the pressure gradient force. Although the flow area reduces at low flow rates, the fluid still travels at speeds that do not generate excessive hydraulic resistance. When the flow rate is low, the hole diameter has little impact on MHL.

The bit is propelled forward by back-jetting nozzles. An illustration of how back-jetting nozzle diameter affects MHL is shown in Fig. 9d. The flow rate through a particular nozzle reduces when its diameter is decreased at a constant total flow rate. Consequently, the propulsion force generated by the bit is reduced. MHL declines significantly as a result of this reduction. Additionally, it causes a higher pressure drop across the bit. A 30% reduction in the diameter of the back-jetting nozzles results in a negative MHL. As a result, up to 20% of diameter change is considered in the analysis. While MHL is strongly affected by the diameter reduction, increasing the back nozzle diameter has a limited effect on it. With constant total flow rates, the diameter increase has a limited impact on HML because the impact of the enhanced flow rate through the back-jetting nozzles is limited as a result of the reduced jet velocity. Consequently, the propulsion force, which is determined by the product of flow rate and jet velocity, does not change significantly as the diameter of the back-jetting nozzles increases. The effect is limited since the reduction in velocity is compensated by the increase in flow rate. However, the increase in nozzle diameter slightly reduces the pressure drop, allowing the flow rate to increase.

Current findings regarding RJD technology suggest that it can be applied in geothermal wells, and advancements in direction control and drilling capabilities could make this technology a valuable alternative to hydraulic fracturing. Due to the fact that microholes are drilled without direct mechanical contact with the rock (hydraulic jetting), RJD technology could also revolutionize drilling in hard and abrasive formations.

4. CONCLUSIONS

In a review of recent studies on radial jet drilling, we demonstrate the challenges associated with expanding this technology for geothermal applications. The following conclusions can be drawn from this review study:

- High-pressure downhole conditions make the jetting of hard formations very challenging due to the increased confined compressive strength of rocks.
- For RJD to be effective, it requires trajectory measurement and control techniques that are currently unavailable.
- Due to the strong correlation between operating parameters, bit design, and formation characteristics, more accurate hydraulic models are needed to optimize the jetting process of lateral holes.
- Tubes and hoses used in RJD must have the appropriate flexibility and strength to handle the high pressure required to drill hard geothermal formations while maintaining their flexibility to ensure smooth sliding.

ACKNOWLEDGMENTS

This investigation would not be possible without the University of Oklahoma and Mewbourne School of Petroleum and Geological Engineering support. As a result, we greatly appreciate their support and assistance.

REFERENCES

Balch, R. S., Ruan, T., Savage, M., & Harvard, J. 2016. Field Testing and Validation of a Mechanical Alternative to Radial Jet Drilling for Improving Recovery in Mature Oil Wells. Paper presented at the SPE Western Regional Meeting, Anchorage, Alaska, USA, May 2016. doi: https://doi.org/10.2118/180410-MS.

Cheung J.B., and Hurlburt, G.H. 1979. Submerged water-jet cutting of concrete and granite. In: Proceedings of the third international symposium on jet cutting technology. Chicago; 11-13 May: E5–E49.

Dickinson, W., Anderson, R. R., and R. W. Dickinson. 1989. The Ultrashort-Radius Radial System. SPE Drill Eng 4 (1989): 247–254. doi: https://doi.org/10.2118/14804-PA.

Gorischny, M., Oppelt, J., Reinicke, K.M., Teodoriu, C. 2015. Fishbone Drilling – An Alternative to Hydraulic Fracturing? Celle Drilling 2015 – International Conference & Exhibition for Advanced Drilling Technology, Celle, Germany, September 15-16.

Huang, Z. and Huang, Z. 2019. Review of Radial Jet Drilling and the key issues to be applied in new geo-energy exploitation, Energy Procedia, Volume 158, Pages 5969-5974.

Kolle J.J. 1987. Jet kerfing parameters for confined rock. In: Proceedings of the fourth U.S. Water Jet Conference. Berkeley. 26-28 August, 134–144.

Li, G., Huang, Z., and Li, J. 2017. Study of radial jet drilling key issues; Petroleum Drilling Techniques; 45(02):1-9.

Nair, R., Peters, E., Šliaupa, S., Valickas, R. and Petrauskas, S. 2017. A case study of radial jetting technology for enhancing geothermal energy systems. Paper SGP-TR-212 presented at the 42nd Workshop on GRE, Stanford University.

Reinsch, T., Paap, B., Hahn, S., Wittig, V., and van den Berg, S. 2018. Insights into the radial water jet drilling technology – Application in a quarry, Journal of Rock Mechanics and Geotechnical Engineering, Volume 10, Issue 2, Pages 236-248.

Salimzadeh, S., Grandahl M., Medetbekova, M. and Nick, H.M. 2019. A novel radial jet drilling stimulation technique for enhancing heat recovery from fractured geothermal reservoirs. Renewable Energy, Vol. 139, 395-409.

Schlichting, H, and Gersten, K. 1997. Grenzschicht-Theorie. 9th Ed. Berlin Heidelberg: Springer.

Stoxreiter, T., Martin, A., Teza, D. and Galler, R. 2018. Hard rock cutting with high pressure jets in various ambient pressure regimes. International Journal of Rock Mechanics and Mining Sciences, Vol. 108, 179-188.

Wiechman, A. and Ahmed, R. 2018. Hydraulic Force Modeling of Radial Jet Drilling. Paper AADE-18-FTCE-008 presented at the 2018 AADE Fluids Technical Conference.

Wiechman, A. and Ahmed, R. M. 2022. A Generalized Hydraulic Model for Propulsion Force Calculations in Radial Jet Drilling. SPE Drilling & Completion, 1-17.

Zhang, S., Huang, Z., Huang, P., Wu, X., Xiong, C., and Zhang, C. 2018. Numerical and experimental analysis of hot dry rock fracturing stimulation with high-pressure abrasive liquid nitrogen jet. Journal of Petroleum Science and Engineering. Volume 163, Pages 156-165.